EUROPEAN ORGANIZATION FOR NUCLEAR RESEARCH

Proposal to the ISOLDE and Neutron Time-of-Flight Committee

Collective isovector valence-shell excitations in the N=84 isotone ^{138}Xe

January 9, 2025

H. Mayr[1], V. Werner[1], N. Pietralla[1], T. Stetz[1], U. Ahmed[1], F. Browne[2], K. Gladnishki[3], K. E. Ide[1], D. Kocheva[3], Th. Kröll[1], S. Meyer[1], C. M. Nickel[1], G. Rainovski[3], N. Warr[4,5], R. Zidarova[1]

[1] *Institut für Kernphysik, Technische Universität Darmstadt, Darmstadt, Germany*
[2] *University of Manchester, Manchester, United Kingdom*
[3] *Sofia University St. Kliment Ohridski, Sofia, Bulgaria*
[4] *Institut für Kernphysik, Universität zu Köln, Cologne, Germany*
[5] *Oliver Lodge Laboratory, University of Liverpool, Liverpool, United Kingdom*

Spokespersons: V. Werner (vw@ikp.tu-darmstadt.de), H. Mayr (hmayr@ikp.tu-darmstadt.de)
Contact person: C. Porzio (carlotta.porzio@cern.ch)

CERN-INTC-2025-012 / INTC-P-735
09/01/2025

Abstract: It is proposed to investigate the evolution of collective isovector valence-shell excitations in the N=84 isotonic chain by unambiguously identifying the lowest-energy mixed-symmetry 2^+ state of ^{138}Xe from its enhanced $M1$ decay rate. The enhanced $B(M1; 2^+_{1,\mathrm{ms}} \rightarrow 2^+_1)$ transition strength will be measured in a Coulomb-excitation experiment. Therefore, a ^{138}Xe radioactive ion beam with an energy of 500 MeV provided by HIE-ISOLDE will impinge on a ^{206}Pb target. This reaction will ensure the population of the 2^+_3 state which is the most probable candidate for the first mixed-symmetry 2^+ state. The Miniball array will be used for γ-ray detection and a double-sided silicon-strip detector will be placed in forward beam direction to set particle-γ conditions.

Requested shifts: 15 shifts

1 Motivation and physics case

Atomic nuclei are mesoscopic two-fluid quantum systems and exhibit complex dynamics governed by collectivity, shell structure, and isospin degrees of freedom. The interplay and balance of these three nuclear phenomena can be studied through quadrupole-collective valence-shell excitations, which result from the mixture of the underlying pure proton and neutron excitations. The isoscalar part of the quadrupole-collective excitations can be described by an in-phase combination of proton and neutron contributions. The corresponding configuration is called fully symmetric. An isovector configuration, in which the oscillation of valence protons and valence neutrons is out of phase, is called mixed-symmetric configuration [1, 2]. The interaction of protons and neutrons in the valence shell of even-even nuclei determines the structure and characteristics of mixed-symmetry states (MSSs). The structure of the isoscalar and the isovector one-phonon valence-shell quadrupole excitations and the interrelation between their wave functions are particularly apparent in their Q-phonon formulation

$$|2_1^+\rangle \propto (Q_\pi + Q_\nu)\,|0_1^+\rangle = Q_s|0_1^+\rangle\,, \quad (1)$$

$$|2_{1,ms}^+\rangle \propto (Q_\pi - \alpha Q_\nu)\,|0_1^+\rangle = Q_m|0_1^+\rangle\,, \quad (2)$$

where the (positive) parameter α ensures the orthogonality of these one-phonon wave functions.

The proton-neutron symmetry of the wave functions of excited states can be quantified in the nuclear shell model by the analysis of the relative signs of the basis states' contributions to the $E2$ and $M1$ decay matrix elements [3, 4, 5]. Figure 1 exemplarily shows the phase difference between proton and neutron contributions to the fully- and mixed-symmetric 2^+ states of ^{132}Te. In algebraic models, such as the Interacting Boson Model-2 (IBM-2) the symmetry of the respective wave functions is quantified by the F-spin [1, 6]. MSSs represent an entire class of collective excitations, with the one-quadrupole phonon $2^+_{\mathrm{ms},1}$ state being the lowest-lying configuration for heavy vibrational nuclei [1]. This $2^+_{\mathrm{ms},1}$ state can be experimentally identified by its distinct signatures [7]. The most unique feature is a strong $M1$ transition to the lowest-energy fully-symmetric state, the 2^+_1 state. The weakly collective E2 ground-state transition is another distinct observable of the $2^+_{\mathrm{ms},1}$ state and makes it possible to access this particular state by Coulomb excitation.

MSSs, thus, allow to access and quantify the building blocks of nuclear collectivity. By an analysis of their shell model wave functions, they allow to determine the fundamental quadrupole-collective configurations of valence protons and neutrons for a given region of the nuclear chart. MSSs have been observed in stable and radioactive nuclei, most commonly in the mass A≈90 region [8, 9, 10, 11, 12, 13, 14], and most recently in the mass A≈208 region [15, 16, 17]. Furthermore, in the region around the doubly-magic ^{132}Sn, the evolution of the $2^+_{\mathrm{ms},1}$ state has been investigated in the N=80 isotonic chain for Z=52-60 [18, 19, 20, 21, 22]. Our new results on ^{132}Te allowed to assign the mixed-symmetry character to the 2^+_2 state of this neutron-rich nuclide [5] through a direct lifetime measurement with the Doppler shift attenuation method in a two-neutron transfer reaction at the 9 MV FN Pelletron tandem accelerator at IFIN-HH in Bucharest. On the proton-rich side of the so-far investigated N=80 isotones, we identified the $2^+_{\mathrm{ms},1}$ state of ^{142}Sm for the first time through the measurement of the B(M1;$2^+_{\mathrm{ms},1} \rightarrow 2^+_1$) strength in a

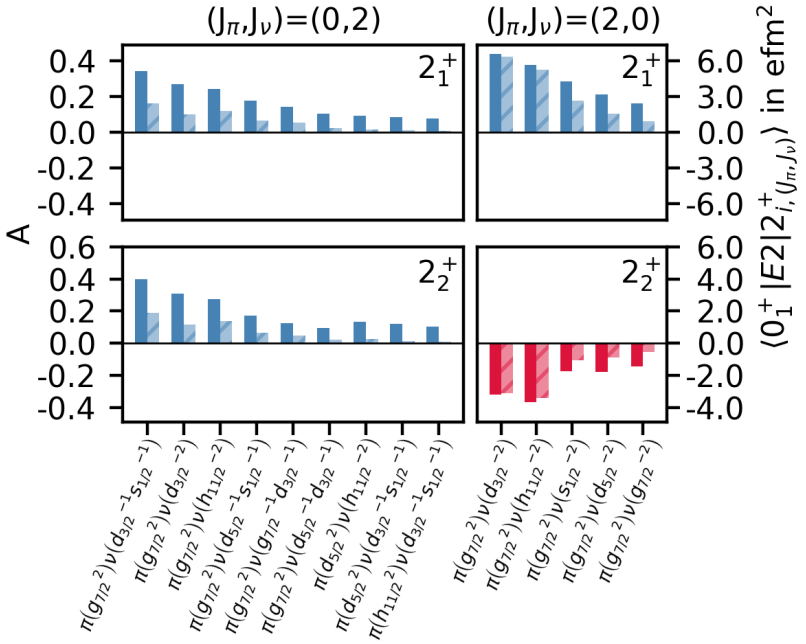

Figure 1: Amplitudes of leading components of the wave functions (solid bars) of the fully-symmetric 2_1^+ state (top) and the mixed-symmetry 2_2^+ state (bottom) of ^{132}Te are shown [5]. The contributions correspond to coupling of either proton or neutron pairs to $J_{\pi,\nu}$=2. Contributions of the proton and neutron parts to the $\langle 0_1^+|E2|2_{1,2}^+\rangle$ matrix elements are denoted by the hatched bars. Positive signs are marked in blue and negative signs in red.

Coulomb-excitation experiment performed at HIE-ISOLDE [23, 24]. In addition, we have measured the missing multipole mixing ratio of the $2_3^+ \rightarrow 2_1^+$ transition from $\gamma\gamma$-angular correlations following β-decay [24]. That measurement was performed at the Heavy Ion Laboratory in Warsaw, Poland. It revealed an almost pure $2_3^+ \rightarrow 2_1^+$ $M1$ transition and confirms the 2_3^+ state as the main component of the $2_{\mathrm{ms},1}^+$.

One motivation for the systematic studies of the first mixed-symmetry 2^+ state in the N=80 isotonic chain was to quantify the robustness of the F-spin symmetry and to reveal the restoration of F-spin symmetry above Z=58. Breaking of the F-spin symmetry can be observed in ^{138}Ce, where the $2_{\mathrm{ms},1}^+$ state is strongly mixed with a nearby 2^+ state, observed from the distribution of the corresponding $M1$ transition strength over several excited 2^+ states. This observation is in contrast to the neighboring isotopes in the N=80 isotonic chain, in which a single well-pronounced one-phonon MSS has been observed, i.e. ^{132}Te [18], ^{134}Xe [19], ^{136}Ba [20], ^{140}Nd [22], and most recently ^{142}Sm [23]. This phenomenon is known as shell stabilization [28]. Different theoretical approaches employing the quasiparticle-phonon model (QPM) [32] and the large-scale shell model [33] have shown, that the fragmentation of the first mixed-symmetry 2^+ state in ^{138}Ce is caused by the underlying shell structure. In particular the Z=58 subshell closure was found to impact the $M1$ strength concentration of the quadrupole-collective isovector valence-shell excitation [28]. The observation of only one 2^+ state with the decay behavior that is ex-

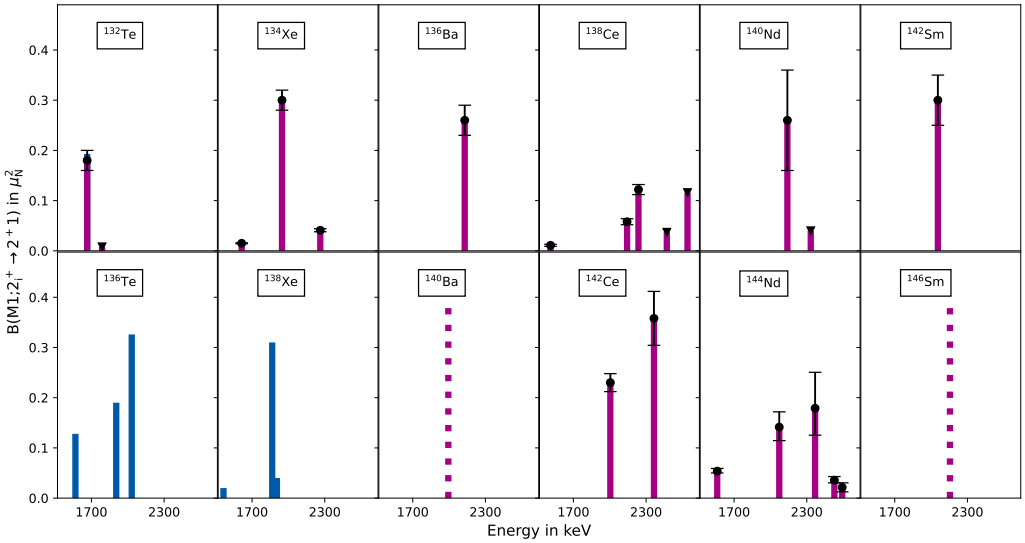

Figure 2: The B(M1;$2_i^+ \rightarrow 2_1^+$) of N=80 (top) and N=84 (bottom) isotones is shown. The $2^+_{\mathrm{ms},1}$ state of ^{138}Ce, ^{142}Ce and ^{144}Nd is clearly fragmented. The position for the expected energy of the $2^+_{\mathrm{ms},1}$ state of ^{140}Ba and ^{146}Sm is marked by dashed lines. Shell model calculations are depicted in blue. In the case of ^{132}Te, the theoretical B(M1;$2_i^+ \rightarrow 2_1^+$) [25] is hardly visible since it agrees very well with the value from the experiment. While the shell model calculation for ^{136}Te [25] predicts a highly fragmented $2^+_{\mathrm{ms},1}$, our calculation with the jj56pnb interaction results in a high concentration of the $M1$ transition strength in the 2_3^+ state of ^{138}Xe. Experimentally obtained values for N=80 have been taken from Refs. [5, 26, 27, 28, 29, 24]; for N=84 from Refs. [30, 31].

pected for the $2^+_{\mathrm{ms},1}$ state in ^{136}Ce indicates that the neutron degrees of freedom strongly influence the fragmentation of the $2^+_{\mathrm{ms},1}$ state [34, 35].
The comparison of the $2^+_{\mathrm{ms},1}$ and the first fully-symmetric 2_1^+ state allows to identify the fundamental quadrupole-collective configurations. Fragmentation of the $2^+_{\mathrm{ms},1}$ indicates a strong orbital dependency of the proton-neutron quadrupole-quadrupole interaction. Therefore, the investigation of MSSs and their fragmentation are suited to test theoretical models. However, experimental data on MSSs in the rare-earth region is scarce. To obtain information on MSSs in the N=82-126 shell, the best approach is to study the N=84 isotonic chain with two valence neutrons. The examination of the particle-hole symmetry may resolve whether the Z=58 sub-shell closure has an identical influence on the robustness of the F-spin above N=82 as it does below the shell closure. Experimentally only little is known about the N=84 isotones. Little data exists for ^{142}Ce [36, 30, 37]: neutron-scattering data and most recently photon scattering [38]. Vanhoy *et al.* have shown, that the $M1$ strength of the $2^+_{\mathrm{ms},1}$ state of ^{142}Ce is split over the 2_3^+ and 2_4^+ state [30]. Using the same technique, the MSSs of ^{144}Nd have also been investigated [31]. Here, a fragmentation of the $2^+_{\mathrm{ms},1}$ state was observed, as shown in Figure 2. Assuming the fragmentation of the $2^+_{\mathrm{ms},1}$ state of ^{142}Ce is mainly a result of the underlying proton sub-shell structure, the fragmentation of the $2^+_{\mathrm{ms},1}$ state of ^{144}Nd indicates no isotonic shell

stabilization.
In the N=84 isotonic chain only the highly fragmented MSSs of ^{142}Ce and ^{144}Nd are known to date. Since the mid-subshell nuclide ^{134}Xe has the most pronounced $2^+_{\mathrm{ms},1}$ in the N=80 isotones, it is of particular interest to investigate if the $M1$ strength is also concentrated in a single 2^+ state in its isotopic counterpart across the neutron shell closure, i.e. ^{138}Xe. Shell model calculations predict such a strong $M1$ transition between the 2^+_3 state and the 2^+_1 state (see Figure 2). Therefore, ^{138}Xe is an ideal candidate to extend the study of the F-spin symmetry to the N=84 chain.
MSSs in ^{138}Xe have not been extensively experimentally investigated so far. Nevertheless, information about the $2^+_{\mathrm{ms},1}$ state in ^{138}Xe is of utmost importance for the investigation of shell stabilization in the N=84 isotonic chain. The 2^+_2 has been investigated in a β-decay experiment at ILL, France [39]. Results from this experiment show a predominant $E2$ character of the $2^+_2 \rightarrow 2^+_1$ transition and it can therefore be concluded, that the 2^+_2 state of ^{138}Xe is not the $2^+_{\mathrm{ms},1}$ state.
Shell model calculations with the NuShellX code [40] have been performed with standard effective charges of $e_p = 1.5$ and $e_n = 0.5$. Effective spin g-factors of $g_{sp} = 3.234$, $g_{sn} = -2.083$ and effective orbital g-factors of $g_{lp} = 1.107$, $g_{ln} = -0.065$ have been used. It can be seen in Figure 3 that the theoretical calculations reproduce the known experimental level scheme well, including the $E2$ transition strength of the first 2^+ state to the ground state which is within the uncertainty of the experimental value [41]. The largest deviation from the experimental values is the underestimation of the branching ratio of the 4^+_2. Generally, the calculations reliably reproduce the known experimental observables and therefore might also be trustworthy for unknown values. The calculations predict an $M1$ transition strength mainly concentrated in the 2^+_3 state of ^{138}Xe. Using the jj56pnb interaction [42] which assumes a ^{132}Sn core, N3LO and takes Coulomb interaction into account, the $M1$ transition strength is expected to be $\mathrm{B(M1;}2^+_3 \rightarrow 2^+_1) = 0.31\,\mu_N^2$. While the 2^+_2 and 2^+_4 states are predicted to carry only $\sim 10\%$ of the $M1$ transition strength to the 2^+_1 each compared to the 2^+_3 state.
It is interesting to note that for the neighboring isotope ^{136}Te shell model calculations by Otsuka *et al.* [25] predict a strong fragmentation of the $M1$ transition strength, while its concentration in a single 2^+ state is well reproduced for ^{132}Te. Also the heavier $N = 84$ Ce and Nd isotones show a strong fragmentation of the $2^+_{\mathrm{ms},1}$ as the experimental data in Figure 2 shows. In contrast, the present shell model calculation for ^{138}Xe predicts the concentration of the $M1$ transition strength in the 2^+_3 state.
Close to the predicted 2^+_3 energy of ^{138}Xe, at 1866 keV, a state with spin assignment $J^\pi = (1, 2^+)$ is known [43], which fulfills the expected decay behavior of the searched $2^+_{\mathrm{ms},1}$ state. Assuming $J^\pi = 2^+$ for this state, we propose to measure the $\mathrm{B(M1;}2^+_3 \rightarrow 2^+_1)$ strength. Due to the low-energy transition of the next potential 2^+ state at 1903 keV with $J^\pi = (2^+, 3, 4^+)$, and its weak branching ratio to the 2^+_1 state of $\mathrm{I}_{2^+\rightarrow 2^+_1}/\mathrm{I}_{\mathrm{tot}} \approx 0.35$, that state can be ruled out as the main fragment of the $2^+_{\mathrm{ms},1}$ state of ^{138}Xe. Based on this information and the comparison to ^{140}Ba, it is suspected that the $2^+_{\mathrm{ms},1}$ character of ^{138}Xe is predominantly concentrated in the 2^+_3 state. Another literature $(1, 2^+)$ state at 2115 keV decays significantly to the 2^+_2 state, which is not expected for the $2^+_{\mathrm{ms},1}$ state. Hence, the mixed-symmetry character is likely to be concentrated in a single state, the 1866-keV state of ^{138}Xe. This we will put to a test, in particular in light of the above-mentioned

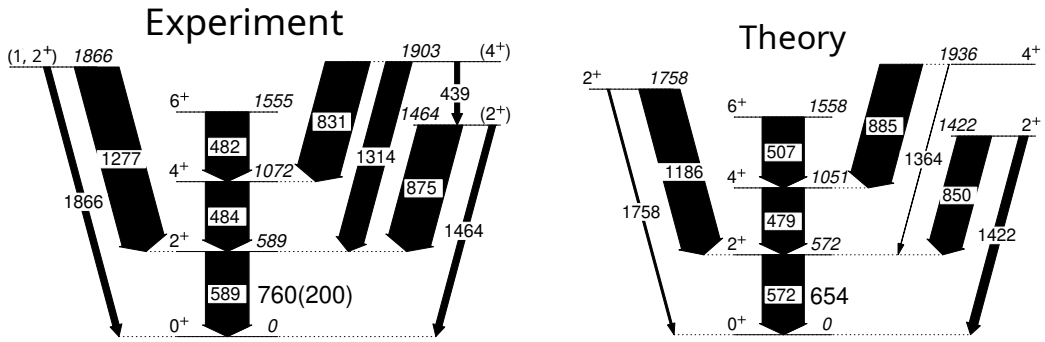

Figure 3: Comparison of experimental (left) and theoretical (right) level scheme. The theoretical calculations were performed with the NuShellX code [40] using the jj56pnb interaction [42]. It can be seen that the calculations reproduce the experimentally [43, 44] obtained levels, including spin and parity quantum numbers and energies, very well. The largest deviation can be seen for the second 4^+ state with underestimation of the transition to the first 2^+ and neglecting the decay to the second 2^+. $E2$ transition strengths from the $2^+_1 \rightarrow 0^+_1$ transition are shown next to the decay arrow in e^2fm^4 [41].

fragmentation of the $2^+_{ms,1}$ state in neighboring isotopes.
With its significant $E2$ matrix element to the ground state, the 2^+_3 state of the neutron-rich unstable ^{138}Xe is well accessible through Coulomb excitation. An experiment to populate low-lying excited 2^+ states of ^{138}Xe has to be performed at a radioactive ion beam facility, where the beam can be produced with sufficient intensity. The intense radioactive ^{138}Xe ion beam necessary for this measurement has been used at HIE-ISOLDE before. In combination with the high-resolution detector array Miniball [45] we will be able to measure the excitation strength of the MSSs candidates through observation of the two decays to the 2^+_1 and 0^+_1 states.

2 Experimental details

Summary of requested shifts: 15 shifts
We propose to use the well-established technique of sub-barrier Coulomb excitation to extract the electromagnetic matrix elements of transitions between the excited states of ^{138}Xe. The isotope will be produced with a standard uranium carbide target. The beam has been well-developed and used in previous REX-ISOLDE experiments [41]. The isotopes will be extracted from the target with an intensity of $1 \cdot 10^8$ ions/µC. The xenon nuclei will be ionized by the cold plasma ion source and subsequently charge-bred by EBIS. Finally, the ions will be accelerated by HIE-ISOLDE to energies of 3.6 MeV/u. An intensity of around $3 \cdot 10^6$ pps can be expected at Miniball by considering the extraction rate of $1.5 \cdot 10^8$ ions per second for a proton current of 1.5 µA and a typical transmission efficiency of 2%.
We plan to use 2 mg/cm^2 of ^{206}Pb as a secondary target. Both projectile and target nuclei will be excited via Coulomb excitation in the scattering process. The scattered nuclei will be detected by the DSSD, placed about 25 mm behind the target, which will cover angles between approximately 20 and 60 degrees. Safe Coulomb excitation is ensured for all

angles, covered by the particle detector. Kinematics of the reaction can be seen in Figure 4. Deexcitation γ-rays will be detected by the Miniball array.

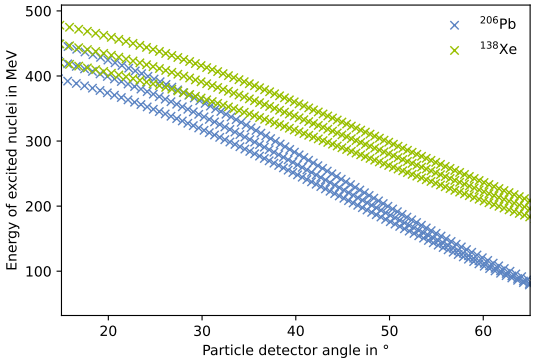

Figure 4: Kinematics of ^{138}Xe at 500 MeV on a ^{206}Pb target. Excitation is assumed at the surface, middle and back of the target.

The electromagnetic matrix elements will be extracted from a fit of the experimentally observed γ-ray yields. The ^{206}Pb target has a 2^+ first excited state at an energy of 803 keV, which has a precisely known reduced transition probability to the ground state, which will be used for normalization.
We want to identify the one-phonon MSS in the N=84 Xe isotope by extracting the $M1$ transition probabilities for the B(M1;$2^+_{\mathrm{ms},1} \rightarrow 2^+_1$) from the experimental yields. The multipole mixing ratio of ^{138}Xe is not available for the $2^+_{\mathrm{ms},1}$ candidate 2^+_3. We plan to measure angular correlations to determine the multipole mixing ratio of the transition of interest in a separate experiment. Estimations of the expected cross sections to excite the 2^+ states of ^{138}Xe have been calculated with CLX [46] using level energies from Ref. [43] and the $2^+_1 \rightarrow 0^+_1$ transition strength from Ref. [41]. For the remaining matrix elements we used the results from our shell model calculations as input. The yields – considering the decay branching ratios – can be found in Table 1.

Table 1: Detected γ-ray yield estimations for depopulation of 2^+ states of ^{138}Xe after Coulomb excitation on a 2 mg/cm^2 ^{206}Pb target. Reaction in the middle of the target is assumed. γ-ray efficiency is taken to be 5% and beam intensity of $3 \cdot 10^6$ pps at Miniball is used for the calculation. Cross sections have been calculated with scattering angles of ^{138}Xe between 20° and 60° by CLX [46].

Excited state	Energy (keV)	σ (mb)	Branching ratio to 2^+_1	Yield/day	Total yield in $4\frac{2}{3}$ days	Statistical uncertainty
2^+_1	588	$2.9{\cdot}10^3$	—	$2.2{\cdot}10^5$	$1.0{\cdot}10^6$	0.1%
2^+_2	1463	8.0	93%	563	2630	2.0%
2^+_3	1866	1.3	87%	85	400	5.0%

We request 14 shifts of data taking. In this time we expect to observe 400 events of the transition of the suspected 2^+_3 state to the 2^+_1 state with a γ-ray energy of 1277 keV. We aim to achieve a statistical uncertainty of around 5% in the peak area of interest. We request an additional shift for beam setup and tuning.

References

[1] F. Iachello. In: *Phys. Rev. Lett.* 53 (1984), p. 1427.

[2] N. Lo Iudice et al. In: *Phys. Rev. Lett.* 41 (1978), p. 1532.

[3] N. Pietralla et al. In: *Nucl. Phys. A* 704.1 (2002), pp. 69–78.

[4] K. Sieja et al. In: *Phys. Rev. C* 80 (5 Nov. 2009), p. 054311.

[5] T. Stetz et al. In: (2024). Submitted to Phys Rev C.

[6] P. Van Isacker et al. In: *Ann. Phys. (N.Y.)* 171 (1986), p. 253.

[7] N. Pietralla et al. In: *Prog. Part. Nucl. Phys.* 60 (2008), p. 225.

[8] N. Pietralla et al. In: *Phys. Rev. Lett.* 83 (1999), p. 1303.

[9] N. Pietralla et al. In: *Phys. Rev. Lett.* 84 (2000), p. 3775.

[10] N. Pietralla et al. In: *Phys. Rev. C* 64 (2001), p. 031301.

[11] C. Fransen et al. In: *Phys. Lett. B* 508 (2001), p. 219.

[12] V. Werner et al. In: *Phys. Lett. B* 550 (2002), p. 140.

[13] C. Fransen et al. In: *Phys. Rev. C* 67 (2003), p. 024307.

[14] S. W. Yates. In: *J. Radioanal. Nucl. Ch.* 265 (2005), p. 291.

[15] D. Kocheva et al. In: *J. Phys. Conf. Ser.* Vol. 724. 2016, p. 012023.

[16] R. Stegmann et al. In: *Phys. Lett. B* 770 (2017), p. 77.

[17] R. Kern et al. In: *Phys. Rev. C* 99 (2019), p. 011303.

[18] M. Danchev et al. In: *Phys. Rev. C* 84 (2011), p. 061306.

[19] T. Ahn et al. In: *Phys. Lett. B* 679 (2009), p. 19.

[20] N. Pietralla et al. In: *Phys. Rev. C* 58 (1998), p. 796.

[21] G. Rainovski et al. In: *Phys. Rev. Lett.* 96 (2006), p. 122501.

[22] R. Kern et al. In: *Phys. Rev. C* 102 (2020), p. 041304.

[23] R. Kern et al. In: *EPJ Web Conf.* Vol. 194. 2018, p. 03003.

[24] T. Stetz et al. In: (2024). Submission in preparation.

[25] T. Otsuka et al. Private Communication. 2024.

[26] T. Ahn et al. In: *Phys. Lett. B* 679.1 (2009), pp. 19–24.

[27] N. Pietralla et al. In: *Phys. Rev. C* 58 (2 Aug. 1998), pp. 796–800.

[28] G. Rainovski et al. In: *Phys. Rev. Lett.* 96 (12 2006), p. 122501.

[29] R. Kern et al. In: *Phys. Rev. C* 102 (4 2020), p. 041304.

[30] J. R. Vanhoy et al. In: *Phys. Rev. C* 52 (1995), p. 2387.

[31] S. F. Hicks et al. In: *Phys. Rev. C* 57 (1998), p. 2264.

[32] N. Lo Iudice et al. In: *Phys. Rev. C* 77 (2008), p. 044310.

[33] K. Sieja et al. In: *Phys. Rev. C* 80 (2009), p. 054311.
[34] T. Ahn et al. In: *Phys. Rev. C* 75 (2007), p. 014313.
[35] T. Ahn et al. In: *Phys. Rev. C* 86 (2012), p. 014303.
[36] W. D. Hamilton et al. In: *Phys. Rev. Lett.* 53 (1984), p. 2469.
[37] W. J. Vermeer et al. In: *Phys. Rev. C* 38 (1988), p. 2982.
[38] A. Gade et al. In: *Phys. Rev. C* 69 (2004), p. 054321.
[39] J. Copnell et al. In: *Z. Phys. A-Hadron. Nucl.* 344 (1992), p. 35.
[40] B. A. Brown et al. In: *Nucl. Data Sheets* 120 (2014), pp. 115–118.
[41] Th. Kröll et al. In: *Eur. Phys. J.-Spec. Top.* 150 (2007), pp. 127–129.
[42] B. A. Brown. Unpublished.
[43] Jun Chen. In: *Nucl. Data Sheets* 146 (2017), pp. 1–386.
[44] A. Korgul et al. In: *Eur. Phys. J. A* 7.2 (Feb. 2000), pp. 167–176.
[45] N. Warr et al. In: *Eur. Phys. J. A* 49.3 (2013), p. 40.
[46] H. Ower. Unpublished.

3 Details for the Technical Advisory Committee

3.1 General information

Describe the setup which will be used for the measurement. If necessary, copy the list for each setup used.

☒ Permanent ISOLDE setup: *Miniball + CD*

- ☒ To be used without any modification
- ☐ To be modified: *Short description of required modifications.*

☐ Travelling setup (*Contact the ISOLDE physics coordinator with details.*)

- ☐ Existing setup, used previously at ISOLDE: *Specify name and IS-number(s)*
- ☐ Existing setup, not yet used at ISOLDE: *Short description*
- ☐ New setup: *Short description*

3.2 Beam production

For any inquiries related to this matter, reach out to the target team and/or RILIS (please do not wait until the last minute!). For Letters of Intent focusing on element (or isotope) specific beam development, this section can be filled in more loosely.

- Requested beams:

Isotope	Production yield in focal point of the separator ($/\mu$C)	Minimum required rate at experiment (pps)	$t_{1/2}$
^{138}Xe	$1 \cdot 10^8$	$3 \cdot 10^6$	14.1 min

- Full reference of yield information
  Production yield information: target team (S. Stegemann)
  Transmission efficiency: HIE-ISOLDE team (A. Rodriguez Rodriguez)
  Assumed proton current: 1.5 µA
- Target - ion source combination: U Carbide + VD7 cold plasma source
- RILIS? *No*
  - ☐ Special requirements: (*isomer selectivity, LIST, PI-LIST, laser scanning, laser shutter access, etc.*)
- Additional features?
  - ☐ Neutron converter: (*for isotopes 1, 2 but not for isotope 3.*)
  - ☐ Other: (*quartz transfer line, gas leak for molecular beams, prototype target, etc.*)
- Expected contaminants: None

- Acceptable level of contaminants:
- Can the experiment accept molecular beams? No
- Are there any potential synergies (same element/isotope) with other proposals and LOIs that you are aware of? No

3.3 HIE-ISOLDE

For any inquiries related to this matter, reach out to the ISOLDE machine supervisors (please do not wait until the last minute!).

- HIE ISOLDE Energy: 3.6 MeV/u
  - ☒ Precise energy determination required
  - ☐ Requires stable beam from REX-EBIS for calibration/setup? No
- REX-EBIS timing
  - ☒ Slow extraction
  - ☐ Other timing requests
- Which beam diagnostics are available in the setup?
  Faraday cup after the target position (XT01.BFC.USER1) and 10-mm active collimator placed 440 mm upstream of the target position (XT01.BFC.USER2).
- What is the vacuum level achievable in your setup? $< 8 \cdot 10^{-7}$mbar

3.4 Shift breakdown

The beam request only includes the shifts requiring radioactive beam, but, for practical purposes, an overview of all the shifts is requested here. Don't forget to include:

- Isotopes/isomers for which the yield need to be determined
- Shifts requiring stable beam (indicate which isotopes, if important) for setup, calibration, etc. Also include if stable beam from the REX-EBIS is required.

Summary of requested shifts:

With protons	Requested shifts
Beam setup ^{138}Xe	1
Data taking, ^{138}Xe	14
Without protons	Requested shifts
Standard source calibration	few hours

3.5 Health, Safety and Environmental aspects

3.5.1 Radiation Protection

- If radioactive sources are required:
  - Purpose: Calibration
  - Isotopic composition: ^{152}Eu, ^{60}Co
  - Activity: Available standard source
  - Sealed

3.5.2 Only for traveling setups

- Design and manufacturing
  - ☐ Consists of standard equipment supplied by a manufacturer
  - ☐ CERN/collaboration responsible for the design and/or manufacturing
- Describe the hazards generated by the experiment:

Domain	Hazards/Hazardous Activities		Description
Mechanical Safety	Pressure	☐	[pressure] [bar], [volume][l]
	Vacuum	☐	
	Machine tools	☐	
	Mechanical energy (moving parts)	☐	
	Hot/Cold surfaces	☐	
Cryogenic Safety	Cryogenic fluid	☐	[fluid] [m3]
Electrical Safety	Electrical equipment and installations	☐	[voltage] [V], [current] [A]
	High Voltage equipment	☐	[voltage] [V]
Chemical Safety	CMR (carcinogens, mutagens and toxic to reproduction)	☐	[fluid], [quantity]
	Toxic/Irritant	☐	[fluid], [quantity]
	Corrosive	☐	[fluid], [quantity]
	Oxidizing	☐	[fluid], [quantity]
	Flammable/Potentially explosive atmospheres	☐	[fluid], [quantity]
	Dangerous for the environment	☐	[fluid], [quantity]
Non-ionizing radiation Safety	Laser	☐	[laser], [class]
	UV light	☐	
	Magnetic field	☐	[magnetic field] [T]
Workplace	Excessive noise	☐	
	Working outside normal working hours	☐	
	Working at height (climbing platforms, etc.)	☐	
	Outdoor activities	☐	
Fire Safety	Ignition sources	☐	
	Combustible Materials	☐	

	Hot Work (e.g. welding, grinding)	□	
Other hazards			